Sepp1[UF] forms are N-terminal selenoprotein P truncations that have peroxidase activity when coupled with thioredoxin reductase-1

Suguru Kurokawa[a], **Sofi Eriksson**[b], **Kristie L. Rose**[c], **Sen Wu**[d], **Amy K. Motley**[a], **Salisha Hill**[c], **Virginia P. Winfrey**[a], **W. Hayes McDonald**[c], **Mario R. Capecchi**[d], **John F. Atkins**[d,e], **Elias S. J. Arnér**[b], **Kristina E. Hill**[a], and **Raymond F. Burk**[a]

[a]Division of Gastroenterology, Hepatology, and Nutrition, Department of Medicine, Vanderbilt University School of Medicine, Nashville, Tennessee 37232 [b]Division of Biochemistry, Department of Medical Biochemistry and Biophysics, Karolinska Institutet, SE- 171 77, Stockholm, Sweden [c]Vanderbilt Proteomics Laboratory in the Mass Spectrometry Research Center, Department of Biochemistry, Vanderbilt University School of Medicine, Nashville, Tennessee 37232 [d]Department of Human Genetics, University of Utah, Salt Lake City, Utah 84112 [e]Department of Biochemistry, University College Cork, Cork, Ireland

To whom correspondence should be addressed: Raymond F. Burk, Department of Medicine/GI, Vanderbilt University School of Medicine, 1030C Medical Research Building IV, Vanderbilt Medical Center, Nashville, TN 37232-0252, USA. Tel: 615-343-4748; Fax: 615-343-6229; raymond.burk@vanderbilt.edu.

Footnote

[1]Abbreviations:

apoER2	apolipoprotein E receptor-2
Gpx	glutathione peroxidase
LC-MS/MS	liquid chromatography-coupled tandem mass spectrometry
PBS	phosphate-buffered saline
PCT	proximal convoluted tubule
Sepp1	selenoprotein P
Sepp1[UF]	selenoprotein P urinary fragments
t-BuOOH	*tert*-butyl hydroperoxide
Trx1	thioredoxin-1
TrxR1	thioredoxin reductase-1
U	selenocysteine

Abstract

Mouse selenoprotein P (Sepp1) consists of an N-terminal domain (residues 1-239) that contains 1 selenocysteine (U) as residue 40 in a proposed redox-active motif (-UYLC-) and a C-terminal domain (residues 240-361) that contains 9 selenocysteines. Sepp1 transports selenium from the liver to other tissues by receptor-mediated endocytosis. It also reduces oxidative stress *in vivo* by an unknown mechanism. A previously uncharacterized plasma form of Sepp1 is filtered in the glomerulus and taken up by renal proximal convoluted tubule (PCT) cells via megalin-mediated endocytosis. We purified Sepp1 forms from the urine of *megalin*$^{-/-}$ mice using a monoclonal antibody to the N-terminal domain. Mass spectrometry revealed that the purified Urinary Sepp1 consisted of N-terminal Fragments terminating at 11 sites between residues 183 and 208. It was therefore designated Sepp1^{UF}. Because the N-terminal domain of Sepp1 has a thioredoxin fold, Sepp1^{UF} was compared with full-length Sepp1, Sepp1$^{\Delta 240-361}$, and Sepp1^{U40S} as a substrate of thioredoxin reductase-1 (TrxR1). All forms of Sepp1 except Sepp1^{U40S}, which contains serine in place of the selenocysteine, were TrxR1 substrates, catalyzing NADPH oxidation when coupled with H_2O_2 or *tert*-butyl hydroperoxide as the terminal electron acceptor. These results are compatible with proteolytic cleavage freeing Sepp1^{UF} from full-length Sepp1, the form that has the role of selenium transport, allowing Sepp1^{UF} to function by itself as a peroxidase. Ultimately, plasma Sepp1^{UF} and small selenium-containing proteins are filtered by the glomerulus and taken up by PCT cells via megalin-mediated endocytosis, preventing loss of selenium in the urine and providing selenium for the synthesis of glutathione peroxidase-3.

Keywords

selenoprotein P forms; selenium homeostasis; extracellular peroxidase activity; selenium-containing proteins; megalin

Introduction

Selenoprotein P (Sepp1)[1] is an extracellular glycoprotein that is made up of an N-terminal, thioredoxin-fold domain containing a single selenocysteine residue in a redox motif and a smaller C-terminal domain containing multiple selenocysteines—9 in humans and mice. The selenium-rich C-terminal domain endows Sepp1 with a selenium transport function and the N-terminal domain is postulated to function as a redox enzyme (1).

Most research on Sepp1 has focused on the function of its C-terminal domain in regulating whole-body selenium and in transporting selenium from the liver to peripheral tissues (2-4). Genomic analysis and research reports indicate, however, that the N-terminal domain also functions *in vivo*—probably as an antioxidant enzyme (5-8). It is not clear whether the full-length Sepp1 form exerts both these functions or whether forms of Sepp1 are produced to exert each function.

Zebrafish (and several other species) have two Sepp1 genes—one for the N-terminal domain alone (presumed antioxidant function) and one for the full-length protein (selenium transport function) (9). In most animals, however, including humans and mice, there is only one gene for Sepp1. These observations raise the question of whether the single Sepp1 gene in most species can be the source of two (or more) protein forms of Sepp1.

Over a decade ago, our group detected "isoforms" of rat Sepp1 that terminated at selenocysteine residues (10) This finding raised the possibility that these forms exert distinct functions. In a subsequent *in vitro* study, however, doubt was cast on the physiological significance of these forms when inefficient read-through of in-frame UGAs in Sepp1 mRNA was shown to produce similar truncated Sepp1 forms (11). Thus, the biological

significance of plasma Sepp1 forms that terminate at selenocysteine positions is questionable.

In vitro evidence has been presented that shortened forms of Sepp1 can be produced from the full-length protein. Proteases of the kallikrein family cleaved full-length human SEPP1 into N-terminal and C-terminal fragments (12), raising the possibility that proteolytically generated forms of Sepp1 exist *in vivo.*

Identification and characterization of naturally occurring Sepp1 forms would likely lead to better understanding of Sepp1 physiology and function. Sepp1 forms are present in vesicles within renal PCT cells, indicating that they are taken up from the glomerular filtrate (13). Moreover, their presence in the glomerular filtrate implies that they are smaller than full-length Sepp1 and might be a modified form of that protein.

Megalin, also known as Lrp2, is a member of the low-density lipoprotein receptor family and is present on the brush border of renal PCT cells. It binds proteins present in the glomerular filtrate and facilitates their endocytosis (14). This process prevents urinary loss of filtered plasma proteins, including Sepp1 forms (15).

Sepp1 has been studied in mice with mutated *megalin* (15). Most of the ligand-binding region of megalin was deleted in those mice and they excreted Sepp1 forms in their urine as had been expected. Little characterization of those Sepp1 forms was reported, but loss of Sepp1 in the urine was shown to predispose the mice to becoming selenium deficient.

Because characterization of the Sepp1 forms in the urine of *megalin*$^{-/-}$ mice might provide insight into Sepp1 metabolism and function, we raised mice that lack megalin entirely and characterized N-terminal Sepp1 forms that appeared in their urine. Those forms—like full-length Sepp1—had peroxidase activity when coupled with TrxR1 and NADPH. Thus Sepp1 is processed *in vivo* to free its enzymatically active N-terminal domain.

Material and methods

Reagents

Oligonucleotides were obtained from core lab facilities at the University of Utah and at Vanderbilt University Medical Center (Molecular Cell Biology Resources Core). ^{75}Se-labeled sodium selenite (specific activity >250 Ci/g selenium) was purchased from the University of Missouri Research Reactor Facility (Columbia, MO). NADPH was purchased from USB Corporation. Glutathione reductase was purchased from Sigma. Recombinant rat TrxR1 (27-28 U/mg) was expressed and purified as described elsewhere (16). Recombinant human thioredoxin-1 (Trx1) was a gift from Dr. Arne Holmgren (Karolinska Institutet, Stockholm, Sweden). All other chemicals were of reagent grade.

Production of Sepp1^{U40S} mice and partial characterization of purified Sepp1^{U40S}

This is the first report of the *Sepp1*^{U40S} mouse with serine replacing selenocysteine at residue 40. Because the purified protein Sepp1^{U40S} was used in this study to assess the importance of the selenocysteine at residue 40 for the redox activity of Sepp1, we are presenting the methods used to produce the mice and limited characterization of Sepp1^{U40S} protein.

The designation *Sepp1*^{U59S} is used for the construction of the mutant gene because nucleotide triplets are counted from the start of the 19-amino acid signal peptide. The mice and the resulting protein use the designation Sepp1^{U40S} for consistency with the other

mutant of this protein, Sepp1$^{\Delta240\text{-}361}$ (17) that does not include the signal peptide in counting the amino acid residues.

Construction of *Sepp1*^{U59S} targeting vector. To construct the targeting vector, a method described previously was followed (18). Recombineering was used to subclone a 13.1 kb genomic fragment from a BAC clone RP23-41H17, which was obtained from BACPAC resources (http://bacpac.chori.org/). The two oligos used in this step (WS785 and WS786) are shown in Table 1. The resulting plasmid from this step was named pStartK-Sepp1. PCR-based mutagenesis was used to convert the DNA encoding the first selenocysteine from TGA to TCA, which encodes serine. The self-excising neo selection cassette ACN was inserted at the BglI site before the second exon. The resulting plasmid was named pStartK-Sepp1U59SACN. To add a negative selection HSV-tk gene, Gateway recombination was performed to quickly transfer Sepp1U59SACN into an HSV-tk containing vector named pWSTK2. The resulting targeting vector was named pWSTK2-Sepp1U59SACN.

Generation of *Sepp1*^{U40S} mice. Standard electroporation of the linearized targeting vector into ES cells was performed as previously described (18). Southern blot analysis was performed to identify correctly targeted ES cell clones. The 5' Southern probe template (476 bp) was amplified by PCR from the BAC clone RP23-41H17 with primers WS869-5F and WS870-5R (Table 1). DNA isolated from ES cells was digested with BamHI, and run on a 0.9% agarose gel. Southern blot was done with the 5' probe. The wild-type band is 15.7 kb, and the targeted mutant band is 6.9 kb. The positive targets were further confirmed by Southern blot analysis with XbaI digest using the 5' probe. Targeted ES cells were injected into blastocysts using our standard protocol. Male chimeric mice were bred with C57BL/6 females to obtain the desired *Sepp1*^{U40S} allele. Since we used the self-excising neo cassette ACN, the neo was automatically deleted in the F1 generation of heterozygotes. The University of Utah Institutional Animal Care and Use Committee approved animal protocols used to generate the mutant mouse. Adult *Sepp1*$^{U40S/+}$ mice (mice heterozygous for the serine mutation allele) were transferred to the animal facility at Vanderbilt University. At Vanderbilt, male and female mice homozygotic for substitution of serine at the first selenocysteine position (*Sepp1*$^{U40S/U40S}$) were determined to be fertile. These mice were bred with C57BL/6J mice to produce a congenic *Sepp1*$^{U40S/U40S}$ breeding colony.

Animal Husbandry

Male C57BL/6-congenic *megalin*$^{+/-}$ mice (kindly provided by Dr. Joachim Herz of the University of Texas Southwestern Medical Center) were backcrossed 4 times with female FVB/NJ mice (Jackson Lab stock #001800) in order to produce viable *megalin*$^{-/-}$ mice, as suggested to us by Dr. Ulrich Schweizer of the University of Bonn (Germany). The first 409 pups that survived to be weaned were all genotyped and 4.6% were *megalin*$^{-/-}$ mice. There were 9 males and 10 females and all of them had a deformity of the forehead as had been observed in *megalin*$^{-/-}$ mice when they were first produced (19). In subsequent litters, genotyping was carried out only when at least one pup had the forehead deformity. Pups were ear-notched and genotyped by PCR. PCR primer sequences are shown in Table 2. The backcrossed *megalin*$^{+/-}$ male and female mice were used as breeding pairs and their pups were genotyped. *Megalin*$^{-/-}$ pups and their *megalin*$^{+/+}$ littermates were used for experiments.

Sepp1$^{iJ240\text{-}361/+}$ pairs were mated to produce *Sepp1*$^{iJ240\text{-}361/iJ240\text{-}361}$ mice (17). This strain and the *Sepp1*$^{U40S/U40S}$ mice yielded mutant plasma Sepp1 forms that were studied for redox activity.

Mice were housed in plastic cages. The light:dark cycle was 12 h:12 h. Pelleted diet and tap water were provided *ad libitum*. Experimental diets were formulated by Harlan-Teklad to

our specifications (20). The diets were *Torula* yeast-based and were supplemented with selenium as sodium selenite. The basal (selenium-deficient) form of this experimental diet contained less than 0.01 mg selenium/kg (n=7). Sodium selenite was added to the basal diet during mixing to give added selenium concentrations of 0.25 mg/kg (selenium-adequate or control diet) and 1 mg/kg (high-selenium diet for *Sepp1$^{\Delta240-361/\Delta240-361}$* mice lacking the selenium-transporting C-terminal domain of Sepp1). The Vanderbilt University Institutional Animal Care and Use Committee approved studies conducted at Vanderbilt.

Study of Sepp1 forms and Gpx3 present in the urine of megalin$^{-/-}$ mice

Megalin$^{-/-}$ and *megalin$^{+/+}$* mice were housed in metabolic cages with free access to food and water. Urine was collected on ice and stored at −80°C. Pooled urine samples from *megalin$^{-/-}$* mice and pooled urine samples from *megalin$^{+/+}$* mice were dialyzed overnight against PBS at 4°C to remove small-molecule selenium compounds. Dialyzed urine samples were centrifuged for 15 min at 1200 *g* and passed through a 0.2 micron syringe filter. The filtrate was applied to a monoclonal antibody (9S4 against Sepp1) column (13) or to a polyclonal-antibody (against Gpx3) column (21). 9S4-binding Sepp1 fragments were eluted from the 9S4 column and Gpx3 was eluted from the anti-Gpx3 column with 0.1 M glycine, pH 2.5. The flow-through fractions that did not bind to the columns were saved for further study.

In a separate experiment, a tracer dose of ^{75}Se-labeled selenite (15 μCi) was injected intraperitoneally into each mouse. ^{75}Se-labeled urine was collected for 24 h following the injection. After urine collection, each mouse was anesthetized with isoflurane and blood was collected from the inferior vena cava and treated with disodium EDTA (1 mg/ml) to prevent coagulation. Plasma was separated by centrifugation and stored at −80°C.

Radioactive urine proteins were separated by SDS-PAGE. The 15% gel was stained with Coomassie blue and dried. The dried gel was exposed to Kodak BioMax film for detection of ^{75}Se-labeled proteins. Non-radioactive urine was separated on a 10% Bis-Tris NuPAGE gel (Invitrogen) for mass spectrometric analysis.

Selenium content of dialyzed urine and of proteins eluted from 9S4 and anti-Gpx3 columns was determined. The protein-containing solutions obtained from the columns were concentrated using an Amicon Ultra centrifugal filter with molecular weight cut off of 3 kDa (Millipore Corporation).

Mass spectrometry of selenoproteins

Native and deglycosylated Sepp1 protein forms that had been purified from urine and plasma were resolved via SDS-PAGE. The gel was stained with colloidal Coomassie and bands of interest were excised from the gel. Bands were sliced into 1 mm^3 gel pieces, and proteins were reduced with dithiothreitol, carbamidomethylated with iodoacetamide, and in-gel digested with trypsin or Glu-C using methods described in (22). Also, as previously described (22), extracted peptides were reconstituted in 0.1% formic acid and were analyzed by LC-MS/MS using an Eksigent NanoLC and Autosampler and a Thermo Scientific LTQ Orbitrap XL or LTQ Orbitrap Velos mass spectrometer. Briefly, the instruments were operated using a data-dependent method with dynamic exclusion enabled. Full scan (m/z 300-2000 or 400-2000) spectra were acquired with the Orbitrap as the mass analyzer (resolution 60,000), and the top 5 (LTQ Orbitrap XL) or top 12 (LTQ Orbitrap Velos) most abundant ions in each MS scan were selected for fragmentation in the LTQ. An isolation width of 2 m/*z*, activation time of 30 ms (LTQ Orbitrap XL) or 10 ms (LTQ Orbitrap Velos), and 35% normalized collision energy were used to generate MS/MS spectra. For peptide identification, tandem mass spectra were searched against a *Mus musculus* subset of the

UniprotKB (www.uniprot.org) protein database. Database searches were performed using a custom version of Sequest (Thermo Scientific) on the Vanderbilt ACCRE Linux cluster and results were assembled in Scaffold 3 (Proteome Software). All searches were configured to include variable modifications of oxidation on methionine and carbamidomethylation on cysteine or selenocysteine. All tandem mass spectra assigned to Sepp1 peptides were manually validated. Plasma Gpx3 was also in-gel digested with trypsin and Asp-N and analyzed by LC-MS/MS as described above.

Whole-body and tissue selenium determination experiments

At weaning, $megalin^{-/-}$ and $megalin^{+/+}$ male mice were fed selenium-adequate diet (supplemented with 0.25 mg selenium/kg) and female mice were fed selenium-deficient diet (no selenium supplement). Four weeks after weaning, the male mice were anesthetized with isoflurane and blood was removed from the inferior vena cava with a syringe and needle. Female selenium-deficient mice tolerated the selenium deficiency without observable debility and were studied 12 weeks after weaning. Blood was treated with disodium EDTA (1 mg/ml) to prevent coagulation. An aliquot of whole blood was taken for selenium assay and the remainder of the blood was centrifuged. Plasma was frozen for assay of selenium biomarkers. Liver, kidney, muscle, testis, and brain were harvested and frozen in liquid nitrogen. The remaining carcass was frozen in liquid nitrogen. Plasma and tissues were stored at -80°C. Whole-body selenium concentration was calculated as the sum of blood, tissue, and carcass selenium contents divided by body weight.

Biochemical measurements

Plasma Sepp1 concentration was determined using an ELISA (17). Gpx activity was determined using a coupled assay with 0.25 mM hydrogen peroxide as substrate (23). Selenium was measured using a modification (24) of the fluorometric assay of Koh and Benson (25). The limit of selenium detection by this assay is 1 ng. Protein concentration was carried out using bicinchoninic acid reagents (Pierce) except as otherwise indicated.

Protein purification

A 9S4 monoclonal antibody column was used to purify Sepp1 forms from plasma and urine. The starting material was plasma from C57BL/6-congenic $Sepp1^{+/+}$, $Sepp1^{\Delta 240-361/\Delta 240-361}$, and $Sepp1^{U40S/U40S}$ mice (male and female) and urine from $megalin^{-/-}$ and $megalin^{+/+}$ mice (male and female). Gpx3 was purified from $megalin^{-/-}$ urine using an anti-Gpx3 column. The column-bound proteins were washed sequentially with PBS and 1 M NaCl in PBS. Then proteins were eluted with 0.1 M glycine, pH 2.5. Glycine-eluted samples were immediately neutralized with 1 M Tris, pH 9.0. The samples were concentrated and buffer-exchanged against PBS using Amicon Ultra centrifugal filters with a 30 kDa molecular weight cut off. Protein concentrations of the purified Sepp1 variants were determined by absorbance at 280 nm using theoretical extinction coefficients for the proteins, *e.g.,* 27,765 $M^{-1}cm^{-1}$ for full-length Sepp1.

Immunofluorescence Microscopy

Mouse kidneys were fixed 1 h at 4°C with 4% formaldehyde in 0.1 M sodium phosphate, pH 7.4. They were then rinsed in phosphate buffer and infiltrated overnight at 4°C in phosphate buffer containing 20% sucrose. The tissue was immersed in Optimal Cutting Temperature Compound (Fisher Scientific), frozen in liquid nitrogen, and stored at −80°C. Cryosections were rinsed with TBST (20 mM Tris–HCl, pH 8.0, 150 mM NaCl, 0.05% Tween 20, 0.025% sodium azide) and blocked with TBST containing 1% bovine serum albumin and 0.1% glycine for 1 hour. Sections were then incubated with rat monoclonal anti-mouse Sepp1 (9S4) and/or rabbit polyclonal anti-megalin primary antibodies (a gift of Dr. Daniel

C. Biemesderfer of Yale University) in blocking solution for 1 h at room temperature. Control sections were incubated with equivalent levels of non-immune rat or rabbit IgG. Sections were washed 3 times for 5 minutes each in TBST and incubated for 1 h with affinity-purified secondary antibodies diluted in blocking solution. These included Cy3-conjugated F(ab')2 mouse anti-rat IgG (Jackson Immunoresearch Laboratories) and Alexa 488-goat anti-rabbit IgG (Invitrogen). Hoechst 33258 was added to the secondary antibody solution. For double antibody staining, additional controls validated that the secondary antibodies only bound to the appropriate primary antibody. Slides were washed 3 times for 5 min with TBST and were mounted in Fluoromount G (Fisher Scientific). Specimens were examined by phase contrast and fluorescence microscopy and images of experimental and control specimens were obtained using identical photographic exposures. The immune-staining experiment was repeated using three animals and the images shown are representative of all replicates.

Sepp1 enzymatic measurements

To determine TrxR1-coupled Sepp1 redox activities, Trx1 or the various forms of Sepp1 (at concentrations of 1 or of 2 μM) were incubated in microwell plates together with 30 nM recombinant rat TrxR1, 200 μM NADPH, and 0.25 or 2.5 mM H_2O_2, 5 or 10 mM t-BuOOH, or 200 μM insulin as the terminal electron acceptor in a final volume of 100 μL. All assays were performed in 50 mM Tris-HCl, pH 7.5, containing 2 mM EDTA. The reactions were carried out at approximately 22°C and were initiated by the addition of NADPH, whereupon absorbance at 340 nm was followed for either 10 or 30 min. The NADPH extinction coefficient ($6,220$ $M^{-1}cm^{-1}$) was used to calculate moles of NADPH consumed. We used the following approximations of molecular weights to convert protein values to μmoles: 40,692 Da for Sepp1, 27,053 Da for Sepp1 $^{\Delta240-361}$, 40,629 Da for Sepp1^{U40S}, and 23,436 Da for Sepp1^{UF}. These values are the theoretically maximal peptide molecular weights for each of the Sepp1 forms. Reaction mixtures containing everything except the Sepp1 form or Trx1 served as background controls and rates obtained with them were subtracted from the rates presented. Each assay was performed at least twice.

Results

Characterization of selenium distribution in megalin$^{-/-}$ mice

In figure 1A, megalin is present on the apical membranes of renal PCT cells and Sepp1 is present inside renal PCT cells near the glomerulus but not in all megalin-containing PCT cells (presumably not in the more distal ones). In *megalin*$^{-/-}$ mice neither megalin nor Sepp1 can be seen in any PCT cells (Fig 1B). The absence of Sepp1 forms from the more distal PCT cells strongly suggests that Sepp1 forms are completely removed from the glomerular filtrate by megalin-mediated endocytosis and imply that deletion of megalin would lead to excretion of the filtered Sepp1 forms in the urine.

Megalin$^{-/-}$ male mice fed selenium-adequate diet (0.25 mg selenium/kg) maintained a whole-body selenium concentration indistinguishable from that of *megalin*$^{+/+}$ mice (Fig 2A). However, kidney selenium concentration fell to 62% of that in *megalin*$^{+/+}$ mice and plasma Gpx activity fell to 32% (Fig 3A). These findings indicate that loss of Sepp1 and other selenium-containing proteins in the urine caused by deletion of *megalin* (shown below) did not lead to selenium deficiency in the mouse when adequate selenium (approximately twice the mouse dietary selenium requirement of 0.1-0.15 mg/kg) was supplied by the diet, but it did cause localized selenium deficiency in the kidney. Gpx3 is synthesized in kidney PCT cells (26) and secreted into the plasma, so loss of Sepp1 uptake by PCT cells in *megalin*$^{-/-}$ mice likely impaired their ability to synthesize Gpx3 and, thus, lowered plasma Gpx activity.

To assess the effect of megalin when selenium supply is limiting, we studied selenium deficiency in *megalin*$^{-/-}$ mice. Female mice were used for this experiment because we were able to produce only a limited number of *megalin*$^{-/-}$ mice and the male mice that had been produced had been used in other experiments. Figure 2B shows that *megalin*$^{-/-}$ female mice had a lower whole-body selenium concentration than *megalin*$^{+/+}$ female mice when both had been fed selenium-deficient diet for 12 weeks. Selenium concentrations of other tissues were lower in the *megalin*$^{-/-}$ mice than in the *megalin*$^{+/+}$ mice with the kidney level being disproportionately lower than selenium levels in other tissues. All plasma selenium biomarkers were depressed by deletion of *megalin* in selenium-deficient mice (Fig 3B). Weight gain was not affected in selenium-deficient mice by *megalin* deletion (not shown) and no obvious neurological impairment was observed in the selenium-deficient *megalin*$^{-/-}$ mice, although detailed neurological testing was not performed. These findings confirm that loss of megalin, with consequent excretion of Sepp1 forms and other selenium-containing proteins in the urine, exacerbates dietary selenium depletion in tissues (15) with the greatest effect being in kidney.

Appearance of Sepp1 fragments and other selenium-containing proteins in megalin$^{-/-}$ urine

Because PCT cell uptake of Sepp1 from the glomerular filtrate was not detected in *megalin*$^{-/-}$ mice (Fig 1B), we sought Sepp1 forms in mouse urine after the mice had been labeled with tracer doses of ^{75}Se. Figures 4A and 4B show, respectively, an autoradiogram and a Coomassie blue stain of the same gel of urine samples. Lanes 1 and 3 were loaded with urine from *megalin*$^{+/+}$ and *megalin*$^{-/-}$ mice, respectively. Several bands of ^{75}Se are visible in lane 3 but no ^{75}Se bands are seen in lane 1. The urine samples were dialyzed overnight against PBS to remove small-molecule ^{75}Se and loaded onto lanes 2 and 4 according to the amount of ^{75}Se present in each (see figure legend). In lane 2, no distinct ^{75}Se bands are present but the predominant protein band at ~20 kDa was greatly accentuated (Fig 4B) because a greater amount of sample was applied than in lane 1. That protein band presumably represents 'mouse urinary protein,' a normal constituent of mouse urine (27). ^{75}Se bands are present in lane 4 at the same positions as bands in lane 3, indicating that the ^{75}Se in those bands was non-dialyzable. These results confirm that proteins containing selenium were present in the urine of *megalin*$^{-/-}$ mice but were not detectable in the urine of *megalin*$^{+/+}$ mice (15).

The nature of the urinary proteins containing ^{75}Se was investigated. Figures 4C and 4D are, respectively, an autoradiogram and a Coomassie blue stain of a gel containing fractions of the ^{75}Se-labeled *megalin*$^{-/-}$ urine along with plasma from *megalin*$^{+/+}$ and *megalin*$^{-/-}$ mice. Lane 1 contains dialyzed urine from a *megalin*$^{-/-}$ mouse (same sample as lane 4 in Figs 4A & 4B). The dialyzed *megalin*$^{-/-}$ mouse urine was passed over a monoclonal antibody (9S4) column that binds the N-terminal domain of Sepp1. The flow-through of that column is seen in lane 2 and the material that bound to the column beads is seen in lane 3. Two ^{75}Se bands are present in lane 3 between the 25 and 37 kDa markers, indicating the presence of N-terminal Sepp1 forms smaller than the full-length plasma Sepp1 seen to migrate at 50 kDa (lanes 4 & 5). A ^{75}Se band is present at 22 kDa in the flow through (lane 2) and corresponds to the ^{75}Se band representing Gpx3 in plasma (lanes 4 & 5). In a separate experiment (not shown), the 22 kDa ^{75}Se band in urine bound to an anti-Gpx3 column. An additional broad ^{75}Se band that did not bind to either antibody column is present between approximately 12 and 17 kDa (lanes 1 & 2, Fig 4C). This band corresponded to visible protein staining (lanes 1 & 2, Fig 4D), indicating that this ^{75}Se is present in a relatively large amount of protein. This ^{75}Se band was not characterized in detail. These findings demonstrate that Sepp1 forms containing the N-terminal domain and Gpx3 forms are present in the urine of *megalin*$^{-/-}$ mice.

The selenium content of Sepp1 and Gpx3 forms isolated from *megalin*^{−/−} urine was determined. After dialysis, centrifugation, and filtration, urine was passed over antibody columns for purification of Sepp1 and Gpx3. In duplicate experiments, eluted Sepp1 fractions contained 17% and 18% of the selenium in pre-column urine (Table 3). Selenium content per protein molecule was calculated to be 0.67 and 0.62 atoms based on Sepp1 molecules with termination after residue 207 (peptide weight of 23,436 Da) (Fig 5). Selenium eluted from the anti-Gpx3 column was below 0.02% of that in pre-column urine (Table 3). These findings indicate that a significant fraction of dialyzed *megalin*^{−/−} urine selenium—more than 18% when purification yield is taken into consideration—was present as N-terminal Sepp1 forms but that Gpx3 forms, while detected when Gpx3 was labeled by [75]Se (Fig 4C), accounted for very little selenium. A further conclusion that can be reached from these experiments is that most of the protein-bound selenium in the *megalin*^{−/−} urine was present in proteins other than Gpx3 and Sepp1 forms with an intact N-terminal domain.

Mass spectrometric characterization of selenoprotein gel bands from megalin^{−/−} urine

The two bands of urinary Sepp1 forms, positions of which are depicted in lane 3 of figure 4C, were analyzed by LC-MS/MS after digestion with trypsin and with Glu-C (Fig 5A). Coverage of the upper band ended with residue 207 and coverage of the lower band ended with residue 202. These collective fragments have been given the designation Sepp1[UF] (The UF superscript signifies urinary fragments.).

In further analyses of the mass spectrometric results, we sought peptide termination sites not expected to occur with the proteases used for digestion. Figure 5A shows that 10 non-tryptic termination sites were identified in the tryptic digest. They occurred between residues 183 and 208. All the same termination sites were found in the Glu-C digest. However, the non-tryptic termination found after residue 183 was at a Glu-C cleavage site and therefore was expected in the Glu-C digest. In addition, a non Glu-C termination site identified after residue 189 was at a tryptic cleavage site and therefore was expected in the trypsin digest. Thus, the Sepp1 fragments terminate at 11 different sites within a 25-residue stretch. These results indicate that at least 11 N-terminal Sepp1 fragments are excreted in the urine of *megalin*^{−/−} mice, likely accounting for the heterogeneity of the Sepp1[UF] observed in figure 4C.

After isolation from C57BL/6 mouse plasma with a monoclonal antibody (9S4) column and SDS-PAGE, native Sepp1 and its deglycosylated form were subjected to LC-MS/MS analysis. Figure 5B shows that 94% coverage was achieved, indicating that full-length Sepp1 was present in mouse plasma. It was not detected in *megalin*^{−/−} urine, however.

The band identified as Gpx3 by antibody binding was further characterized by LC-MS/MS after trypsin and Asp-N digestions. Coverage of the Gpx3 amino acid sequence was 82%, extending to within 3 residues of the predicted N terminus and 2 residues of the predicted C terminus (Fig 6). These findings suggest that the form of Gpx3 present in the urine was full length.

Purified Sepp1[U40S] produced 3 bands on SDS-PAGE (lane 3 in Fig 7) compared to one band produced by Sepp1 (lane 1 in Fig 7). The top Sepp1[U40S] band migrated the same distance as wild-type Sepp1. The other 2 bands migrated farther, suggesting that those proteins had less mass than the protein in band one.

Mass spectrometric analysis of all 3 Sepp1[U40S] bands showed that serine was present at residue 40 in place of the selenocysteine present in wild-type Sepp1. The bands that migrated farther were forms with C-terminal truncations (results not shown). Thus, replacing

the selenocysteine at residue 40 with serine causes truncation of some, but not all, Sepp1^{U40S} molecules. More detailed characterization of the *Sepp1^{U40S}* mice and the Sepp1^{U40S} protein will be presented in a future report.

Redox activity of Sepp1 forms purified from plasma and megalin$^{-/-}$ urine

Because the putative Sepp1 active site has a thioredoxin-like redox motif with selenocysteine replacing one of its cysteines (Fig 5), all our Sepp1 forms (Fig 7) were studied in a thioredoxin activity assay system (28). NADPH and TrxR1 were used to reduce the Sepp1 form; H_2O_2, *t*-BuOOH, and insulin were used as terminal electron acceptors.

The Sepp1 forms with the redox motif intact had significant peroxidase activities that were similar on a molar basis, but Sepp1^{U40S}, the form with its presumed redox motif disrupted, had essentially no activity (Figs 8A & 8B). These findings indicate that the Sepp1 forms present *in vivo* can serve as substrates of TrxR1. Moreover, these forms have peroxidase activity that is dependent on their selenocysteine-containing redox motif.

Trx1, the usual TrxR1 substrate, had low direct peroxidase activity in this assay system (Figs 8A & 8B). However, it reduced disulfides in insulin, a reaction that was not supported by the Sepp1 forms (Fig 8C). Thus, even though the *in vivo* Sepp1 forms are substrates of TrxR1, their enzymatic activities are different from those of Trx1.

Discussion

This report demonstrates that Sepp1^{UF} is an *in vivo* form of Sepp1. Its diversion in *megalin$^{-/-}$* mice from endocytosis by renal PCT cells to urinary excretion implies that it enters the urinary stream in the glomerulus via filtration of plasma.

Properties and formation of Sepp1^{UF}

Mass spectrometric analysis of Sepp1^{UF} revealed that it consists of 11 N-terminal Sepp1 fragments (Fig 5A). Six of the terminations occur after residues 185-190 and 3 occur after residues 200-202. Thus, 9 of the 11 terminations occur in 2 "hot spots" and the other 2 terminations are nearby. This finding can be explained by proteolytic processing of Sepp1 being the origin of Sepp1^{UF}. It is also possible that some of the termination sites are produced by removal of amino acid residues from longer forms after proteolysis at one or more sites.

Sepp1 has several properties that might influence such proteolytic processing. It binds to cells at 2 sites. One site depends on its heparin-binding property (29,30) and that site is likely to be the heparin-binding site in the N-terminal domain (residues 79-86) (31). The other site is an apoER2-binding site in the C-terminal domain (30). It can be speculated that binding of Sepp1 to cells would make the Sepp1^{UF} termination sites accessible to proteases. Also, because the C-terminal domain associates with the receptor apoER2, proteolytic cleavage might free that domain for endocytosis via apoER2 (32), leaving the N-terminal domain in the extracellular space.

Two highly basic stretches of Sepp1 sequence might also play roles in Sepp1^{UF} production. Seven of the 11 Sepp1^{UF} termination sites are present within or adjacent to a cluster of 8 basic amino acids (within the stretch of residues 185-194) and the other 4 are slightly downstream between residues 200 and 208 (Fig 5A). A second cluster of 10 basic amino acids (within the stretch of residues 223-236) is present downstream of the Sepp1^{UF} termination sites (Fig 5B). Two similar stretches of basic amino acids—mostly histidines—are conserved among species and are potential sites for association of Sepp1 with other proteins, *e.g.,* proteases. This speculative proteolytic process could underlie the presence of

Sepp1^{UF} in the urine of *megalin*$^{-/-}$ mice. Additional work will be necessary to determine the fate of the Sepp1 C-terminus.

A German group observed that the urine of megalin-mutant *(Lrp2*$^{267/267}$*)* mice, in which most of the extracellular domain of megalin was missing, contained Sepp1 forms (15). Using western blots of electrophoresis gels, they observed Sepp1 forms migrating where Sepp1^{UF} migrates. However, they did not characterize those Sepp1 forms further. They also observed a Sepp1 band that migrated with plasma Sepp1. We did not detect such full-length (plasma) Sepp1 in *megalin*$^{-/-}$ mouse urine (Figs 4 & 5A) and, moreover, would not expect it to be filtered in the glomerulus because of its large size (33). These differences between our findings and those of the German group might stem from a difference between *Lrp2*$^{267/267}$ mice and *megalin*$^{-/-}$ mice, although both were on similar mixed (FVB/NJ and C57BL/6) backgrounds.

Significance of megalin-mediated uptake of Sepp1^{UF} and other selenium-containing proteins by renal PCT cells

Selenium is transferred from the liver to other tissues by receptor-mediated endocytosis of Sepp1. While the receptor apoER2 is responsible for Sepp1 uptake by other tissues (30), kidney PCT cells take up Sepp1 forms from the glomerular filtrate via megalin-mediated endocytosis (13). The present report identifies Sepp1^{UF} as a form of Sepp1 taken up in this manner (Fig 5A).

By facilitating PCT cell uptake of selenium-containing proteins, megalin prevents loss of selenium from the body, supporting tissue selenium levels when dietary selenium intake is low (Fig 2B) (15). Moreover, the PCT cells utilize selenium taken up in this manner to synthesize Gpx3, which is secreted into the plasma (26). Thus, megalin plays a role in whole-body selenium metabolism.

In addition to Sepp1^{UF}, Gpx3 and unidentified selenium-containing polypeptides appeared in the urine of *megalin*$^{-/-}$ mice (Fig 4). Thus, PCT cells take up a number of selenium-containing proteins, not just Sepp1^{UF}. The unidentified selenium-containing proteins account for most of the selenium in dialyzed urine (Table 3). Therefore, the role of megalin in selenium metabolism is broader than facilitating uptake of Sepp1^{UF} from the glomerular filtrate. It is even possible that C-terminal fragments of Sepp1 are among the selenium-containing proteins that bind megalin and are taken up by PCT cells. Further insights into whole-body selenium metabolism should be gained by identification of additional selenium-containing proteins in *megalin*$^{-/-}$ urine.

The results of this study allow us to compare and contrast the functions of the Sepp1 receptors apoER2 and megalin. ApoER2 binds to a Sepp1 site in its C terminus and therefore does not bind to Sepp1$^{\Delta240-361}$, which lacks the C-terminal domain (30,34). Megalin, which is a cargo receptor that binds many proteins, appears to bind a number of selenium-containing proteins, including Gpx3 and the Sepp1 N-terminal domain forms Sepp1$^{\Delta240-361}$ (13) and Sepp1^{UF}. It is also possible that megalin binds the C-terminal domain of Sepp1 but more work will be needed to assess that. In addition, we did not assess the possibility that selenium forms bind to cubilin, a ligand-binding protein that is endocytosed through its association with megalin (35).

Peroxidase activity of in vivo Sepp1 forms

Human SEPP1 has been reported to have no Gpx activity with the substrates H_2O_2 and *t*-BuOOH and very low activity, relative to Gpx4, with a phospholipid hydroperoxide substrate (36). This finding of limited Gpx activity and our recognition that the putative

Sepp1 active site at residues 40-43 resembles a thioredoxin active site led us to examine activities of mouse Sepp1 forms when they were coupled with NADPH and TrxR1 instead of with GSH. We found that both *in vivo* Sepp1 forms, Sepp1 and Sepp1^{UF}, have significant peroxidase activity with the substrates H_2O_2 and *t*-BuOOH in the thioredoxin assay system (Fig 8), raising the possibility that they function as peroxidases *in vivo*.

Because Sepp1 and Sepp1^{UF} are extracellular proteins and TrxR1 is an intracellular protein, it is not clear how TrxR1 could reduce oxidized Sepp1 forms, thereby enabling them to function as peroxidases. However, evidence has been presented recently that TrxR1 can be induced to migrate to the exofacial aspect of the cell membrane under stress conditions and to reduce substrates outside the cell using reducing equivalents from intracellular NADPH (37). Sepp1 forms bind to cells through their heparin-binding properties (30) and that would position them near the cell membrane, possibly allowing interaction with membrane-associated TrxR1 and its intracellular NADPH supply. Such a mechanism, while still speculative, might serve to protect the cell membrane from injury by peroxides in the extracellular space. Alternatively, Sepp1 forms might also reduce peroxides in a non-catalytic manner—but that type of activity would be inefficient compared to coupling them with TrxR1.

The role of selenocysteine in accelerating thiol/disulfide exchange reactions is complex (38). The presence of a selenocysteine in the active site of one of the redox partners usually accelerates the thiol/disulfide exchange. The reaction between Sepp1 (or Sepp1^{UF}) and TrxR1 involves active sites that both contain selenocysteines; the occurrence of this reaction strongly suggests that a thiol-selenol can reduce a selenenylsulfide in an appropriate microenvironment. The lack of enzymatic activity of Sepp1^{U40S} when coupled with TrxR1 indicates that the selenocysteine residue present in the other Sepp1 variants was involved in catalyzing the observed peroxidase activity.

Conclusions

We identified Sepp1^{UF} as *in vivo* forms of Sepp1 that are suited to exert an antioxidant function. Sepp1^{UF} lacks the selenium-rich C-terminal domain required for selenium transport but contains the redox-active site and the heparin-binding site. Although important details remain to be clarified, the finding that Sepp1 and Sepp1^{UF} function as peroxidases is a potential explanation for the antioxidant properties of Sepp1. We demonstrated that the selenocysteine-containing redox motif at residues 40-43 is required for this activity and conclude that it is the active site that is reduced by TrxR1 and, in turn, reduces the peroxide substrate.

The demonstration that multiple selenium-containing proteins appear in the urine of *megalin*$^{-/-}$ mice and that megalin binds the N-terminal domain of Sepp1 forms differentiates megalin function from that of apoER2. Megalin facilitates the endocytosis of many filtered proteins, including several selenium-containing ones. ApoER2 is not known to bind any selenium-containing proteins except Sepp1 forms containing the selenium-rich C-terminal domain. Thus, apoER2 functions to supply selenium to extra-hepatic tissues and megalin functions to prevent the loss of small selenium-containing proteins in the urine.

Acknowledgments

References

1. Burk RF, Hill KE. Selenoprotein P-Expression, functions, and roles in mammals. Biochim. Biophys. Acta. 2009; 1790:1441–1447. [PubMed: 19345254]

2. Hill KE, Zhou J, McMahan WJ, Motley AK, Atkins JF, Gesteland RF, Burk RF. Deletion of selenoprotein P alters distribution of selenium in the mouse. J. Biol. Chem. 2003; 278:13640–13646. [PubMed: 12574155]

3. Hill KE, Wu S, Motley AK, Stevenson TD, Winfrey VP, Capecchi MR, Atkins JF, Burk RF. Production of selenoprotein P (Sepp1) by hepatocytes is central to selenium homeostasis. J. Biol. Chem. 2012; 287:40414–40424. [PubMed: 23038251]

4. Schomburg L, Schweizer U, Holtmann B, Flohé L, Sendtner M, Kohrle J. Gene disruption discloses role of selenoprotein P in selenium delivery to target tissues. Biochem. J. 2003; 370:397–402. [PubMed: 12521380]

5. Bosschaerts T, Guilliams M, Noel W, Herin M, Burk RF, Hill KE, Brys L, Raes G, Ghassabeh GH, De Baetselier P, Beschin A. Alternatively activated myeloid cells limit pathogenicity associated with African trypanosomiasis through the IL-10 inducible gene selenoprotein P. J. Immunol. 2008; 180:6168–6175. [PubMed: 18424738]

6. Burk RF, Hill KE, Awad JA, Morrow JD, Kato T, Cockell KA, Lyons PR. Pathogenesis of diquat-induced liver necrosis in selenium-deficient rats. Assessment of the roles of lipid peroxidation by measurement of F_2 isoprostanes. Hepatology. 1995; 21:561–569. [PubMed: 7843731]

7. Lobanov AV, Hatfield DL, Gladyshev VN. Reduced reliance on the trace element selenium during evolution of mammals. Genome Biol. 2008; 9:R62. [PubMed: 18377657]

8. Steinbrenner H, Alili L, Bilgic E, Sies H, Brenneisen P. Involvement of selenoprotein P in protection of human astrocytes from oxidative damage. Free Radic. Biol. Med. 2006; 40:1513–1523.

9. Kryukov GV, Gladyshev VN. Selenium metabolism in zebrafish: multiplicity of selenoprotein genes and expression of a protein containing seventeen selenocyteine residues. Genes Cells. 2000; 5:1049–1060. [PubMed: 11168591]

10. Ma S, Hill KE, Caprioli RM, Burk RF. Mass spectrometric characterization of full-length rat selenoprotein P and three isoforms shortened at the C terminus. Evidence that three UGA codons in the mRNA open reading frame have alternative functions of specifying selenocysteine insertion or translation termination. J. Biol. Chem. 2002; 277:12749–12754. [PubMed: 11821412]

11. Stoytcheva Z, Tujebajeva RM, Harney JW, Berry MJ. Efficient incorporation of multiple selenocysteines involves an inefficient decoding step serving as a potential translational checkpoint and ribosome bottleneck. Mol. Cell. Biol. 2006; 26:9177–9184. [PubMed: 17000762]

12. Saito Y, Sato N, Hirashima M, Takebe G, Nagasawa S, Takahashi K. Domain structure of bi-functional selenoprotein P. Biochem. J. 2004; 381:841–846. [PubMed: 15117283]

13. Olson GE, Winfrey VP, Hill KE, Burk RF. Megalin mediates selenoprotein P uptake by kidney proximal tubule epithelial cells. J. Biol. Chem. 2008; 283:6854–6860. [PubMed: 18174160]

14. Nykjaer A, Dragun D, Walther D, Vorum H, Jacobsen C, Herz J, Melsen F, Christensen EI, Willnow TE. An endocytic pathway essential for renal uptake and activation of the steroid 25-(OH) vitamin D3. Cell. 1999; 96:507–515. [PubMed: 10052453]

15. Chiu-Ugalde J, Theilig F, Behrends T, Drebes J, Sieland C, Subbarayal P, Köhrle J, Hammes A, Schomburg L, Schweizer U. Mutation of megalin leads to urinary loss of selenoprotein P and selenium deficiency in serum, liver, kidneys and brain. Biochem. J. 2010; 431:103–111. [PubMed: 20653565]

16. Xu J, Arnér ES. Pyrroloquinoline quinone modulates the kinetic parameters of the mammalian selenoprotein thioredoxin reductase 1 and is an inhibitor of glutathione reductase. Biochem. Pharmacol. 2012; 83:815–820. [PubMed: 22226931]

17. Hill KE, Zhou J, Austin LM, Motley AK, Ham AJ, Olson GE, Atkins JF, Gesteland RF, Burk RF. The selenium-rich C-terminal domain of mouse selenoprotein P is necessary for supply of selenium to brain and testis but not for maintenance of whole-body selenium. J. Biol. Chem. 2007; 282:10972–10980. [PubMed: 17311913]

18. Wu S, Ying G, Wu Q, Capecchi MR. A protocol for constructing gene targeting vectors: generating knockout mice for the cadherin family and beyond. Nature Protocols. 2008; 3:1056–1076.

19. Willnow TE, Hilpert J, Armstrong SA, Rohlmann A, Hammer RE, Burns DK, Herz J. Defective forebrain development in mice lacking gp330/megalin. Proc. Natl. Acad. Sci. U.S.A. 1996; 93:8460–8464. [PubMed: 8710893]

20. Hill KE, Zhou J, McMahan WJ, Motley AK, Burk RF. Neurological dysfunction occurs in mice with targeted deletion of selenoprotein P gene. J. Nutr. 2004; 134:157–161. [PubMed: 14704310]

21. Olson GE, Whitin JC, Hill KE, Winfrey VP, Motley AK, Austin LM, Deal J, Cohen HJ, Burk RF. Extracellular glutathione peroxidase (Gpx3) binds specifically to basement membranes of mouse renal cortex tubule cells. Am. J. Physiol. Renal Physiol. 2010; 298:F1244–F1253. [PubMed: 20015939]

22. Shonesy BC, Wang X, Rose KL, Ramikie TS, Cavener VS, Rentz T, Baucum AJ 2nd, Jalan-Sakrikar N, Mackie K, Winder DG, Patel S, Colbran RJ. CaMKII regulates diacylglycerol lipase-alpha and striatal endocannabinoid signaling. Nature Neurosci. 2013; 16:456–463. [PubMed: 23502535]

23. Lawrence RA, Burk RF. Glutathione peroxidase activity in selenium-deficient rat liver. Biochem. Biophys. Res. Commun. 1976; 71:952–958. [PubMed: 971321]

24. Sheehan TMT, Gao M. Simplified fluorometric assay of total selenium in plasma and urine. Clin. Chem. 1990; 36:2124–2126. [PubMed: 2253359]

25. Koh TS, Benson TH. Critical re-appraisal of fluorometric method for determination of selenium in biological materials. J. Assoc. Off. Anal. Chem. 1983; 66:918–926. [PubMed: 6885699]

26. Avissar N, Ornt DB, Yagil Y, Horowitz S, Watkins RH, Kerl EA, Takahashi K, Palmer IS, Cohen HJ. Human kidney proximal tubules are the main source of plasma glutathione peroxidase. Am. J. Physiol. 1994; 266:C367–C375. [PubMed: 8141250]

27. Cheetham SA, Smith AL, Armstrong SD, Beynon RJ, Hurst JL. Limited variation in the major urinary proteins of laboratory mice. Physiol. Behavior. 2009; 96:253–261.

28. Arnér ES, Holmgren A. Measurement of thioredoxin and thioredoxin reductase. Curr. Protoc. Toxicol. 2001 Chapter 7:Unit 7.4.1-7.4.14 DOI: 10.1002/0471140856.tx0704s05;

29. Arteel GE, Franken S, Kappler J, Sies H. Binding of selenoprotein P to heparin: Characterization with surface plasmon resonance. Biol. Chem. 2000; 381:265–268. [PubMed: 10782998]

30. Kurokawa S, Hill KE, McDonald WH, Burk RF. Long Isoform Mouse Selenoprotein P (Sepp1) Supplies Rat Myoblast L8 Cells with Selenium via Endocytosis Mediated by Heparin Binding Properties and Apolipoprotein E Receptor-2 (ApoER2). J. Biol. Chem. 2012; 287:28717–28726. [PubMed: 22761431]

31. Hondal RJ, Ma S, Caprioli RM, Hill KE, Burk RF. Heparin-binding histidine and lysine residues of rat selenoprotein P. J. Biol. Chem. 2001; 276:15823–15831. [PubMed: 11278668]

32. Li Y, Lu W, Marzolo MP, Bu G. Differential functions of members of the low density lipoprotein receptor family suggested by their distinct endocytosis rates. J. Biol. Chem. 2001; 276:18000–18006. [PubMed: 11279214]

33. Burk RF, Gregory PE. Some characteristics of ^{75}Se-P, a selenoprotein found in rat liver and plasma, and comparison of it with seleno-glutathione peroxidase. Arch. Biochem. Biophys. 1982; 213:73–80. [PubMed: 7059191]

34. Burk RF, Olson GE, Hill KE, Winfrey VP, Motley AK, Kurokawa S. Maternal-fetal transfer of selenium in the mouse. FASEB J. 2013; 27:3249–3256. [PubMed: 23651543]

35. Christensen EI, Birn H. Megalin and cubilin: multifunctional endocytic receptors. Nature Reviews. Mol. Cell Biol. 2002; 3:256–266.

36. Saito Y, Hayashi T, Tanaka A, Watanabe Y, Suzuki M, Saito E, Takahashi K. Selenoprotein P in human plasma as an extracellular phospholipid hydroperoxide glutathione peroxidase. J. Biol. Chem. 1999; 274:2866–2871. [PubMed: 9915822]

37. Zhang G, Nitteranon V, Guo S, Qiu P, Wu X, Li F, Xiao H, Hu Q, Parkin KL. Organoselenium compounds modulate extracellular redox by induction of extracellular cysteine and cell surface thioredoxin reductase. Chem. Res. Toxicol. 2013; 26:456–464. [PubMed: 23360449]

38. Hondal RJ, Marino SM, Gladyshev VN. Selenocysteine in thiol/disulfide-like exchange reactions. Antioxid. Redox Signal. 2013; 18:1675–1689. [PubMed: 23121622]

Highlights

- Selenoprotein P (Sepp1) has *in vivo* antioxidant properties by an unknown mechanism.

- A form of Seppl is filtered from plasma in the glomerulus and taken up by megalin.

- Seppl[UF], ll Seppl N-terminal fragments, is excreted in the urine of *megalin*^{−/−} mice.

- Seppl[UF] has peroxidase activity when coupled with thioredoxin reductase-l.

- Seppl[UF] might protect cells from injury by extracellular peroxides.
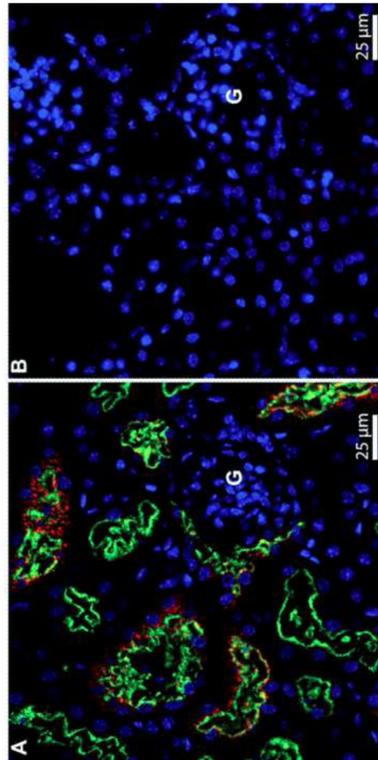
1.
Association of Sepp1 forms (red) with megalin (green) in mouse kidney PCT cells. Panel A depicts *megalin*$^{+/+}$ kidney cortex and panel B depicts *megalin*$^{-/-}$ kidney cortex. G indicates a glomerulus. Cell nuclei are blue.
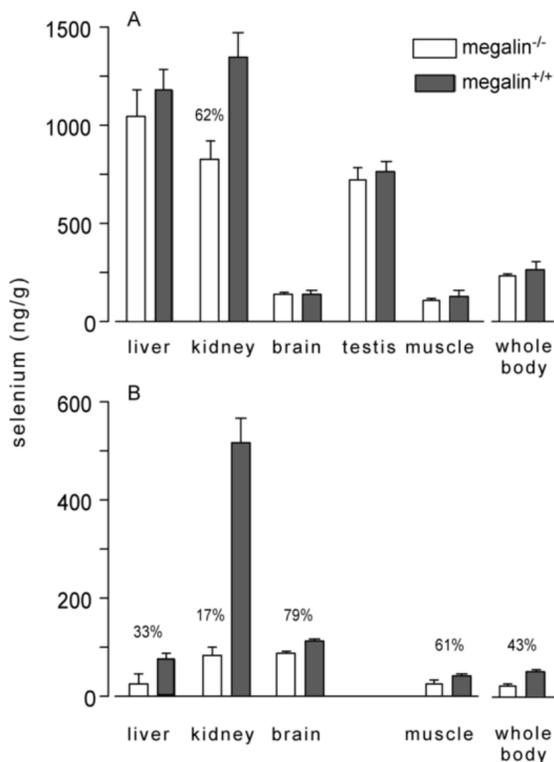
2.
Whole-body and tissue selenium concentrations in *megalin*$^{-/-}$ and *megalin*$^{+/+}$ mice fed (A) selenium-adequate and (B) selenium-deficient diets. Weanling male mice were fed selenium-adequate diet (supplemented with 0.25 mg selenium/kg) for 4 weeks before tissues were taken for analysis. Weanling female mice were fed selenium-deficient diet for 12 weeks before tissues were taken for analysis. Values are means with 1 S.D. indicated by the half bracket, n=5. Pairs were compared using Student's *t*-test and significant differences (p<0.05) are indicated by percentages.
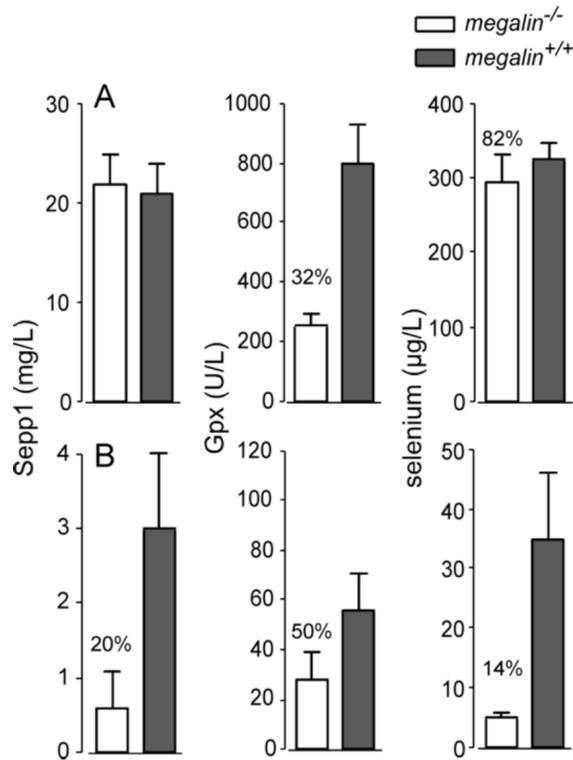
3.

Plasma selenium biomarkers in *megalin*^{−/−} and *megalin*^{+/+} mice fed (A) selenium-adequate diet for 4 weeks and (B) selenium-deficient diet for 12 weeks beginning at weaning. Mice were the same ones presented in figure 2. Values are means with 1 S.D. indicated by half brackets, n=4-5. Pairs were compared using Student's *t*-test and significant differences (p<0.05) are indicated by percentages.
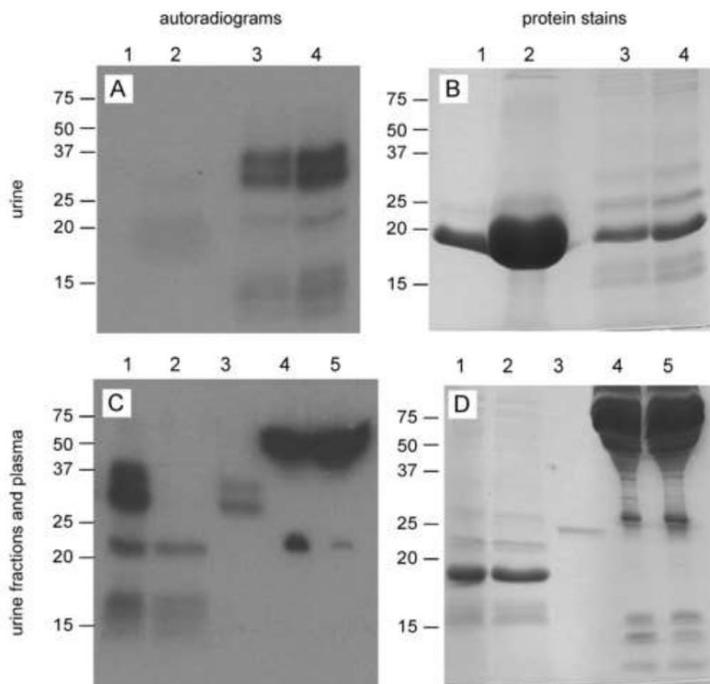
4.
Selenoproteins in the urine of *megalin*^{−/−} and *megalin*^{+/+} mice. Panels A and C are autoradiograms of SDS-PAGE gels of urine and plasma samples from ^{75}Se-labeled *megalin*^{−/−} and *megalin*^{+/+} mice. Panels B and D are the Coomassie stains of the respective gels depicted in panels A and C. Lane 1 in panels A and B was loaded with 1 µl *megalin*^{+/+} urine (1660 cpm ^{75}Se) and lane 2 with 20 µl of the same urine after dialysis (1500 cpm ^{75}Se). Lane 3 was loaded with 5 µl *megalin*^{−/−} urine (2160 cpm ^{75}Se) and lane 4 with 10 µl of the same urine after dialysis (1880 cpm ^{75}Se). Lane 1 in panels C and D was loaded with 10 µl dialyzed *megalin*^{−/−} urine (2060 cpm ^{75}Se). The dialyzed *megalin*^{−/−} urine was passed over a monoclonal antibody (9S4) column that binds the N-terminal domain of Sepp1. The flow through was loaded onto lane 2 and the bound fraction was loaded onto lane 3. Lanes 4 and 5 were each loaded with 1 µl plasma from *megalin*^{+/+} (1890 cpm ^{75}Se) and *megalin*^{−/−} (2170 cpm ^{75}Se) mice, respectively.

A

```
  1 ESQGQSSACY KAPEWYIGDQ NPMLNSEGKV TVVALLQASU
 41 YLCLLQASRL EDLRIKLESQ GYFNISYIVV NHQGSPSQLK
 81 HSHLKKQVSE HIAVYRQEED GIDVWTLLNG NKDDFLIYDR
121 CGRLVYHLGL PYSFLTFPYV EEAIKIAYCE ERCGNCNLTS
161 LEDEDFCKTV TSATANKTAE PSEAHSHHKH HNKHGQEHLG
201 SSKPSEN
```

B

```
  1 ESQGQSSACY KAPEWYIGDQ NPMLNSEGKV TVVALLQASU
 41 YLCLLQASRL EDLRIKLESQ GYFNISYIVV NHQGSPSQLK
 81 HSHLKKQVSE HIAVYRQEED GIDVWTLLNG NKDDFLIYDR
121 CGRLVYHLGL PYSFLTFPYV EEAIKIAYCE ERCGNCNLTS
161 LEDEDFCKTV TSATANKTAE PSEAHSHHKH HNKHGQEHLG
201 SSKPSENQQP GPSETTLPPS GLHHHHRHRG QHRQGHLESU
241 DTTASEGLHL SLAQRKLURR GCINQLLCKL SKESEAAPSS
281 CCCHCRHLIF EKSGSAIAUQ CAENLPSLCS UQGLFAEEKV
321 TESCQCRSPP AAUQNQPMNP MEANPNUSUD NQTRKUKUHS
361 N
```

5.

Mass spectrometric analysis of (A) 9S4-binding Sepp1 fragments from *megalin*^{−/−} urine and (B) Sepp1 purified from plasma. Panel A presents the combined coverage of urinary Sepp1 fragments in the 2 Sepp1 bands between the 37 and 25 kDa markers in lane 3 of figure 4C. The most C-terminal amino acid detected in the upper band was residue 207 and in the lower band it was residue 202. All the amino acid residues shown, except for the 3 in the box, were identified by mass spectrometry. Non-tryptic terminations (❶ over the terminal residue) in a tryptic digest and non Glu-C terminations (⑩ under the terminal residue) in a Glu-C digest were detected, indicating that the 2 bands were mixtures of Sepp1 fragments. The thioredoxin-like putative active site at residues 40-43 is underlined. Panel B presents underlined coverage (93.6%) of Sepp1 purified from C57BL/6 mouse plasma.

```
  1  QEKSKTDCHG  GMSGTIYEYG  ALTIDGEEYI  PFKQYAGKYI
 41  LFVNVASYUG  LTDQYLELNA  LQEELGPFGL  VILGFPSNQF
 81  GKQEPGENSE  ILPSLKYVRP  GGGFVPNFQL  FEKGDVNGEK
121  EQKFYTFLKN  SCPPTAELLG  SPGRLFWEPM  KIHDIRWNFE
161  KFLVGPDGIP  VMRWYHRTTV  SNVKMDILSY  MRRQAALSAR
201  GK
```

6.

Mass spectrometric analysis of protein purified from *megalin*−/− mouse urine using a Gpx3-binding polyclonal antibody column. Digestions were carried out with trypsin and with Asp-N before analysis by mass spectrometry. Amino acids detected by mass spectrometry are underlined.
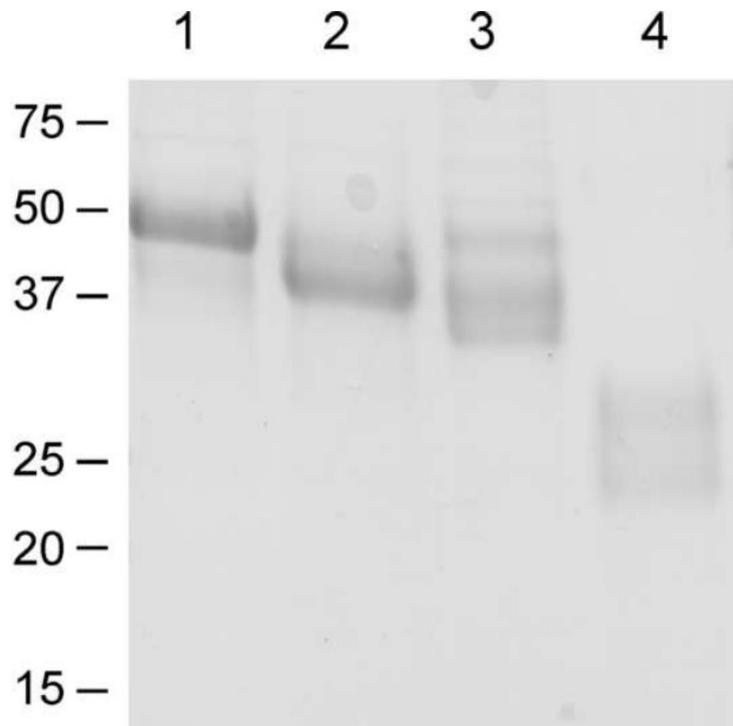
7.
Purified Sepp1 forms used to evaluate redox activity. Sepp1 from C57BL/6 mouse plasma is in lane 1; Sepp1$^{\Delta240\text{-}361}$ from *Sepp1$^{\Delta240\text{-}361/\Delta240\text{-}361}$* mouse plasma is in lane 2; Sepp1^{U40S} from *Sepp1$^{U40S/U40S}$* mouse plasma is in lane 3; and Sepp1^{UF} from *megalin$^{-/-}$* mouse urine is in lane 4. All proteins were purified using a Sepp1-binding monoclonal antibody (9S4) column. The SDS-PAGE was performed on a 15% polyacrylamide gel and 4 µg of each protein preparation was loaded. The proteins were stained with Coomassie blue.
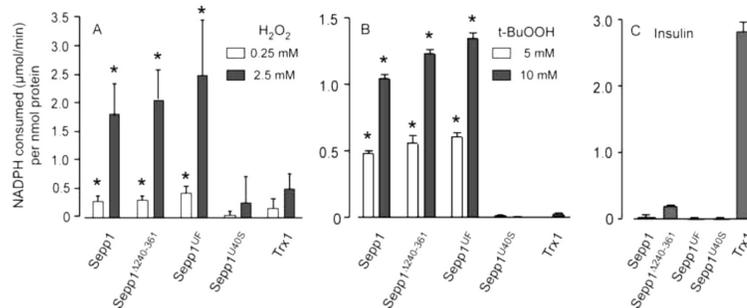
8.

Sepp1 forms containing selenocysteine at residue 40 are substrates of TrxR1 and display peroxidase activity (A & B) but not disulfide reductase activity (C). Bars represent means with 1 S.D. indicated by a bracket. Asterisks indicate values significantly greater ($p < 0.05$) than the respective values (at each H_2O_2 or t-BuOOH concentration) of the Sepp1^{U40S} protein as assessed by ANOVA followed by Tukey's *post hoc* test. The disulfide reductase activities with all forms of Sepp1 (C) were significantly different ($p < 0.05$) from the activity with Trx1.

Table 1

Targeting vector

	primer designation	primer sequence (5'-< 3')
pStartK		
	WS785	GTAGTGCTACTTATAAATCCCAACAGAGTCTCTTT TAGCTGTTGCTTCAGCGACTGAATTGGTTCCTTTA AAGCC
	WS786	ATGTTTATTGCTCACCTAGGCATTATACTAAACAC TCCATGCAAACTACAGCCGCACTCGAGATATCTA GACCCA
Southern blot probes		
	WS869-5F	GAGATCCCAGTAGGTAGGCGACTTG
	WS870-5R	CCTGTAACCTTGAGCCAAACTTCCT

Table 2

PCR primers for genotyping

	primer designation	primer sequence (5'-< 3')	PCR product size (pb)
Sepp1	SePS14	GCCATCAGGGCTCAGTGCAG	wildtype: 600 (SePS14/SePA600)
	SePA600	GGTGTTGGGTCGTTTGTTCGGATCG	
	NeoS2	GGATGCCTGCAGAAGACACAAGTA	homozytote: 500 (SePS14/NeoS2)
Sepp1 $^{\square 240-361}$	MoSePS18	GCAGGAGCATCTTGGCAGCAGT	mutant: 450 wildtype: 370
	MoSePS19	CACTGACAGGATTCAGTGACTTTCTCCT	
Sepp1^{U40S}	WS1004	TCCTAGATTGGCAGAGGATAGAATGAA	mutant: 198 wildtype: 116
	WS1005	TCAGAAACACCTTCCAACTGTAATGC	
megalin	G20	GCACATTTGGCCAGCCAAGG	wildtype: 275 (G20/G21)
	G21	CATATCTTGGAAATAAAGCGAC	
	S175	GATTGGGAAGACAATAGCAGGCATGC	homozygote: 325 (G21/S175)

Table 3

Selenium in selenoproteins purified from *megalin−/−* urine (replicates of the experiment)

seleno-protein	% of the selenium in dialyzed urine	ng selenium/mg protein	nmol selenium/nmol protein (23,436 Da)
Sepp1[UF]	17, 18	2264, 2090	0.67, 0.62
Gpx3	>0.02, >0.02	--	--